DOI: 10.1002/ejic.200500805

Bundle of Nanobelts Up to 4 cm in Length: One-Step Synthesis and Preparation of Titanium Trisulfide (TiS_3) Nanomaterials

Jingjing Ma,[a] Xiaoyang Liu,*[a] Xuejing Cao,[a] Shouhua Feng,[a] and Michael E. Fleet[b]

Keywords: One dimensional / Nanostructures / Layered compounds / Titanium / Sulfides / CVT / One-step synthesis

One-dimensional (1D) titanium trisulfide (TiS_3) nanobelt bundles up to 4 cm in length have been successfully synthesized through an easy and common chemical vapor transition (CVT) process. The as-synthesized samples were characterized by X-ray powder diffraction (XRD), polarized light microscopy, scanning electron microscopy (SEM), and transmission electron microscopy (TEM). All microscopic observations indicated a belt-like morphology. Powder XRD patterns showed that TiS_3 crystallized in the monoclinic system with $a = 4.958(1)$ Å, $b = 3.393(1)$ Å, $c = 8.793(3)$ Å and $\beta = 97.27(5)°$. TEM images revealed a nanostructure with an interplanar spacing of 0.87 nm. The ED pattern and HRTEM images confirmed the [014] elongated direction and the [001] dilated direction of the bundle of TiS_3 nanobelts. Its tensile strength (TS) was further examined with a universal testing machine with 20 N as the biggest strength: the maximum stress and the break strain were 111.027 MPa and 97.1 %, respectively. Because the TiS_3 nanocrystals are up to 4 cm in length and flexible enough to be cut into small pieces, they should be used directly in electrical and electronic applications. Also, these nanomaterials are synthesized and prepared by a simple one-step process.

I. Introduction

Recently, there is a growing interest in the synthesis, characterization, and application of one-dimensional (1D) nanomaterials such as nanobelts, nanowires, etc. because of their low dimensionality and high aspect ratio, as well as their unusual physical properties. The synthesis and functionality of 1D nanomaterials have become one of the most highly energized research areas. During the past two decades, various sulfide nanomaterials have been synthesized.[1–12] However, the preparation of sulfide nanobelts remains poorly studied, and only a few successful examples have been reported. For example, ZnS nanobelts with wurtzite structure have been prepared by simple thermal evaporation of ZnS powder in the presence of Au catalysts at 970 °C.[13] PbS nanobelts have been successfully synthesized in the mixed solution of $PbCl_2$ and $Na_2S_2O_3$.[14]

Titanium trisulfide TiS_3 is of interest to us because of its potential application in CuO-based cathodes of non-aqueous alkali metal batteries. Measurements of the electrical conductivity and the Hall coefficient at 15–300 K and of the thermal EMF at 80–400 K indicate that TiS_3 is semiconducting with extrinsic n-type conductivity. The mobility of the carriers is approximately 30 cm^2/V at room temperature, and increases up to approximately 100 cm^2/V at 100 K, and then drops at lower temperatures.[15] Thin films of TiS_3 have been prepared by thermal chemical vapor deposition (CVD), by reacting $TiCl_4$ and a series of sulfur sources,[16] but the nanoscale synthesis of TiS_3 has few successful results reported. Only Dong-Kyun Seo synthesized the TiS_3 material in the same size with TiO_2 powder and the mixtures of boron and sulfur as starting materials by a solid-gas metathetical reaction,[17] but there was neither SEM nor TEM image to indicate its nanosize. Furthermore, the boron powder could not adsorb all the oxygen completely during this oxidation–deoxidization process, and the remained TiO_2 would reduce the purity of the sample, some other peaks of the mixture from its XRD pattern also confirmed that.

It is well known that the synthesis and preparation generally require two separate steps in the fabrication of functional materials, e.g., firstly the phase is obtained in powder form using different synthesis methods, and then the powder product is processed into different functional forms according to specific applications, with hot pressing being the most common method used to work the powders. However, for nanomaterials, the particle size increases when the nanopowders are hot-pressed, which results in the loss of physical properties associated with the small-size effect (high specific surface area, surface conductivity, etc.). The retention of small particle size while processing the powders into different shapes is a very important issue in the field of nanomaterials. We presently report the synthesis and preparation of high-purity TiS_3 with nanobelt structure by an easy and

[a] State Key Laboratory of Inorganic Synthesis and Preparative Chemistry, College of Chemistry, Jilin University,
2699 Qianjin Street, Changchun, 130012, P. R. China
Fax: +86-431-5168316
E-mail: liuxy@jlu.edu.cn
[b] Department of Earth Sciences, University of Western Ontario, London, Ontario N6A 5B7, Canada

common one-step CVT process, which yields a product that can be used directly in electrical and electronic applications.

II. Results and Discussion

The products were characterized by X-ray diffraction (XRD, with a SIEMENS D5005 diffractometer with a graphite monochromator), scanning electron microscopy (SEM JEOL.LTD JSM-6700F), transmission electron microscopy (TEM, Jeol Ltd., JEM-3010), polarized-light microscopy (Olympus BX51), universal testing machine (Shimadzu AG-I).

The XRD pattern of the bulk samples (e.g., Figure 1) was consistent with pure TiS_3 (JCPDS No. 36–1337). The product crystallized in the monoclinic system with a = 4.958(1) Å, b = 3.393(1) Å, c = 8.793(3) Å and β = 97.27(5)°. The structure calculations were optimized by least-squares refinement. The diffraction peaks were sharp and strong, confirming that the products were well crystallized. This XRD pattern also proved that the [001] direction should be the direction of growth of TiS_3 nanobelts bundle either elongated direction or dilated direction. Using polarized-light microscopy, the TiS_3 crystals were seen to be dark grey with a metallic shine and belt-like habit (Figure 2). The nanocrystals were up to 4 cm in length and, thus, apparently suitable without further treatment as functional material in electrical devices. Figure 2 (c and d) reveal a layered structure in agreement with the strong preferred orientation indicated by the bulk XRD pattern (Figure 1) and the habit of TiS_3 crystals deduced in previous studies.[18,19]

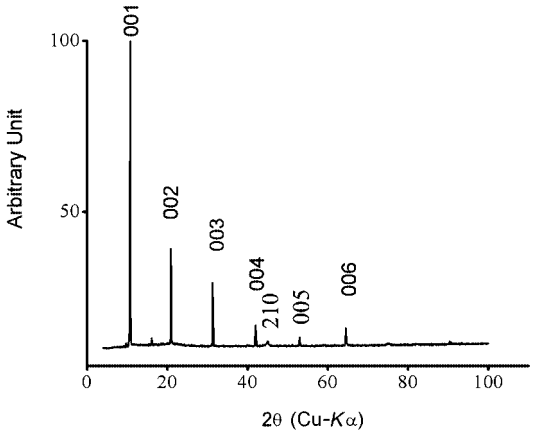

Figure 1. Bulk XRD pattern of the bundle of TiS_3 nanobelts. The numbers above the peaks are the Miller indices for the monoclinic structure.

The morphology of the nanobelt crystals was further investigated by SEM. A typical SEM image of the TiS_3 products (Figure 3, a) shows smooth laminar crystal faces and a layered structure. Figure 3 (b, c and d), shows a more massive habit with individual TiS_3 nanobelts up to 100 μm in length.

TEM images (Figure 4) provide further insight into the morphology of these materials. TiS_3 nanobelts with length

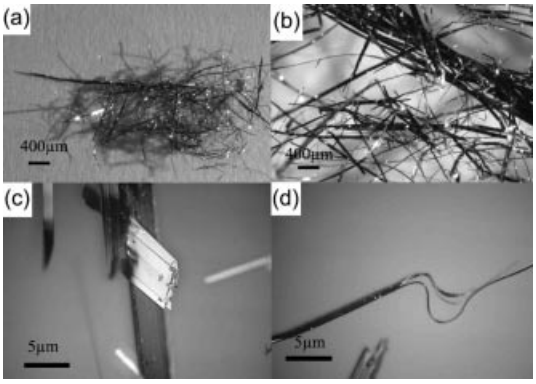

Figure 2. The appearance of the bundle of TiS_3 nanobelts in polarized-light microscopy (Olympus BX51). a) and b) show the dark grey belt-like appearance. c) and d) reveal the layered microstructure.

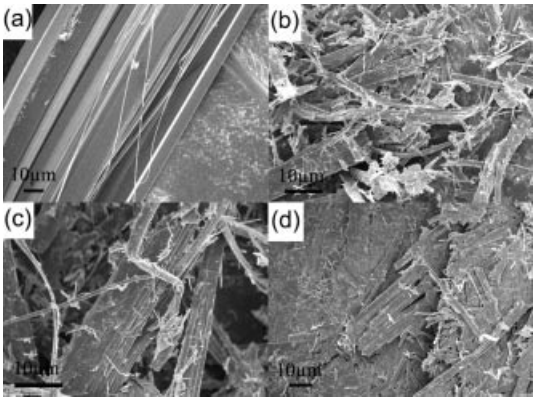

Figure 3. Low-magnification SEM images of TiS_3 nanobelt bundles synthesized by a simple CVT process of Ti and S at 600 °C; a) is taken from the centre of a TiS_3 nanobelt bundle; b) shows the typical appearance of TiS_3 nanobelt bundles; c) and d) show details of massive nanobelts.

up to 4 cm were first comminuted by grinding in ethanol, then the mixed solution was pulsed by ultrasonic cleaner for ca. 10 min. In order to sample the smallest size fraction of TiS_3 crystals, the clear solution on top of the sedimented column was pipetted onto a holey carbon grid, and the ethanol allowed to evaporate. Typical TEM images at low magnification (Figure 4, a and b) show that the ground crystal products are nanobelts, and that the yield of nanobelts is quite high (>95%). The selected-area electron diffraction pattern taken from a single TiS_3 nanobelt confirms the single-crystal nature of the sample and can be indexed on a monoclinic unit cell, consistent with the powder XRD results presented above (JCPDS No. 36–1337). The [014] direction of the ED pattern is parallel to the elongated axis of the belt, showing that the elongated growth might occur along the [014] direction. Furthermore, the [001] direction of the ED pattern is parallel to the dilated axis of the belt, showing that the dilated growth might occur along the [001] direction which corresponds to the XRD result. High-resolution TEM images (Figure 4, c and d) show that the nanobelts are single crystals and free of dislocations and defects.

From Figure 4 (c), we can see that the nanobelts are structurally uniform with an interplanar spacing of 0.87 nm; it should be elongated along the [014] direction and dilated along the [210] direction which is consonant with the ED pattern. The TiS_3 nanobelts were not sensitive to electron beam irradiation during the HRTEM investigation.

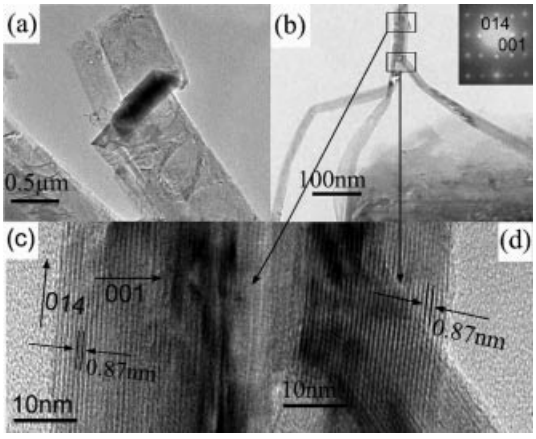

Figure 4. TEM and HRTEM images of the TiS_3 nanobelts revealing details of their geometry; a) and b) are images of several overlapped TiS_3 nanobelts, (inset) The corresponding electron diffraction pattern confirms the single-crystal nature of the sample and can be indexed to a monoclinic unit cell consistent with the XRD results presented above; c) and d) are HRTEM images of a TiS_3 nanobelt, showing that the nanobelts are single crystals and free from dislocations and defects, also, the nanobelts are structurally uniform with an interplanar spacing about 0.87 nm.

Figure 5 shows that in the structure of monoclinic titanium trisulfide TiS_3, two of the three S atoms per formula unit are present as a single-bonded disulfide ion (S_2^{2-}; S–S = 2.04 Å), and the third S atom is formally sulfide (S^{2-}).[16] The Ti atom is in irregular eightfold coordination with S atoms. Six shorter Ti–S distances (2.45 to 2.49 Å) form TiS_6 trigonal prisms, which are linked through shared faces into an infinite chain parallel to the *b*-axis, that makes the structure quasi one-dimensional. Neighboring chains are offset by *b*/2 and connected laterally by longer Ti–S bonds (2.63 and 2.64 Å) into sheets parallel to the crystal face (001). Individual (001) sheets are bounded above and below by a layer of disulfide groups, and held together in the resulting two-dimensional structure by only van der Waals' forces. Extensive bulk and powder XRD[16,18] (Figure 1) and microfocus single-crystal XRD[18] show that the acicular (needle-shaped) and blade- or belt-like crystals of TiS_3 are elongated in a gradient direction, and that the layer surface (i.e., the prominent growth surface) is (001), which is also concluded from HRTEM images and ED pattern. In addition, the TiS_3 nanobelts bundle can be broken into 1D needles, having a parting or cleavage parallel to the (100) direction. This parting is believed to be responsible for the belt-like morphology of the nanocrystals shown in Figure 2 (d) and Figure 4, and requires the severing of the long (2.63 and 2.64 Å) Ti–S bonds. Thus, the broad surface of the nanobelts (Figure 4, a) is a cleavage or parting surface populated by broken bonds, although the strong bonds of the monoclinic TiS_3 structure remain in tact. The nanobelts tend to separate into 1D needles by cleavage along (001), which requires the breaking of the weak van der Waals' bonds. On the basis of this orientational relationship, one would expect that the lattice fringes of Figure 4 (c and d) should correspond to the interlayer spacing d_{001} (0.8706 nm). The 1D TiS_3 needles should get widen layer by layer along the [100] direction which is consistent with the HRTEM results.

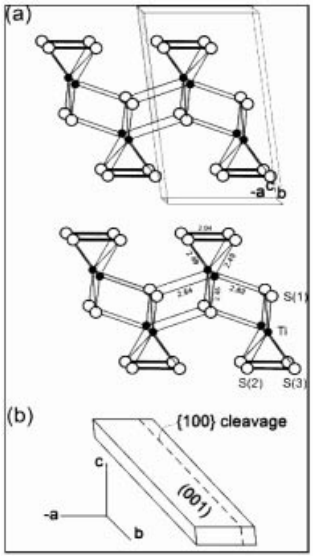

Figure 5. Structure of titanium trisulfide TiS_3; (a) monoclinic structure of titanium trisulfide TiS_3 shows that the Ti atom is in irregular eightfold coordination with S atoms. Six shorter Ti–S distances (2.45 to 2.49 Å) form TiS_6 trigonal prisms, which are linked by shared faces into an infinite chain parallel to the *b*-axis, making the structure quasi one-dimensional; (b) schematic pattern of the layer structure of titanium trisulfide (TiS_3) shows that the crystals of TiS_3 are elongated in the *b*-axis direction and that the layer surface is (001). Also, the crystals have a cleavage parallel to (100).

In order to prove that these bundles of TiS_3 are not extremely fragile, we use an universal testing machine with 20 N as the biggest strength to examine the tensile strength of this material. Figure 6 showed that the maximum stress was 111.027 MPa, the break strain 97.1% and the average stress 100–110 MPa. The maximum stress value of a bundle of TiS_3 is nearly the same with that of aluminum (≈ 100 MPa),[20] and much higher than those of some widely used engineering plastics such as PVC (≈ 25 MPa), poly(propylene) (25.48 MPa)[21] and poly(vinyl acetate) (29.4 MPa),[21] even some films used in conducting application. For example, a poly(*p*-phenylene) (PPP) film was electrochemically deposited onto a stainless steel electrode surface by direct oxidation of benzene in BF_3–diethyl ether solution at an applied potential of 1.7 V (vs. Ag/AgCl), and the as-grown PPP film had a tensile strength of 53.9–63.7 MPa;[22] a crystalline polythiophene (Pth) film was electrochemically deposited onto a nickel substrate from freshly distilled BF_3–diethyl ether (BFEE) solution containing 15 mM thiophene, and the crystalline film had a tensile

strength of 73.5–83.3 MPa.[23] So we believe these TiS_3 nanobelts bundles should be flexible enough to be used in applications directly.

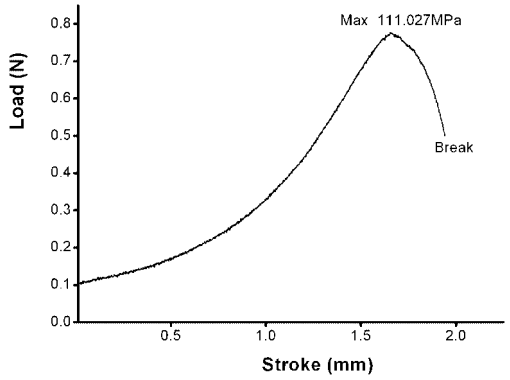

Figure 6. Tensile strength (TS) of the TiS_3 nanobelts bundle.

III. Conclusions

Nanobelt crystals of TiS_3 with sufficient length (≈ 4 cm) and tensile strength (the average stress is 100–110 MPa) to be used directly in electrical devices without further treatment have been produced by a one-step reaction process. The successful synthesis of TiS_3 nanobelts encourages us to investigate the synthesis and preparation of other nanostructured metal sulfides by this easy and common CVT method, which does not require the use of organic (organic sulfur, organometallic) reagents. For the synthetic process, reaction temperature and length of the quartz-glass tube are of great importance. Therefore, establishing these parameters and the relationship between them are key points to the synthesis of metal sulfides with nanostructures. Moreover, the TiS_3 semiconductor nanobelts are expected to present more novel physical properties and applications in practice, and further research is now in progress in our laboratory.

IV. Experimental Section

TiS_3 nanobelt crystals were prepared by the direct reaction of titanium and sulfur within evacuated sealed quartz-glass tubes with a diameter of 10 mm and a length of 130 mm. In order to ensure the purity of the sample, titanium sponge (99.7%; Alfa Aesar) and sulfur sublimate (99.99%; Aldrich) instead of oxides were used as the titanium and sulfur sources, respectively. Charges, consisting of about 1 g of starting composition in the stoichiometric proportion of TiS_3, were loaded in a quartz-glass tube closed at one end using a long-stemmed funnel. Then the tube with the starting materials was evacuated and sealed, and heated in a horizontal-tube furnace. The synthesis was achieved by establishing a temperature gradient of 80–100 °C along the tube with the starting mixture at the hot end. TiS_3 fibers were obtained at the cool end when charges were heated at 600 °C for 15 days. When the temperature was set below 600 °C, the sulfur did not react completely with titanium, and an excess amount of it was deposited at the cool end. Temperatures above 600 °C tended to produce unwanted powder and crystals of TiS_2: TiS_3 undergoes peritectic decomposition (to TiS_2 + native sulfur) at 632 °C, 8.95 atm. The optimum reaction duration was 15 days.

Acknowledgments

This work was supported by the Natural Sciences Foundation of China (No. 20471022) and the Natural Sciences and Engineering Research Council of Canada.

[1] X. Duan, Y. Huang, R. Agarwal, C. M. Lieber, *Nature* **2003**, *421*, 241–245.
[2] C. H. Ye, G. W. Meng, Z. Jiang, Y. H. Wang, G. Z. Wang, L. D. Zhang, *J. Am. Chem. Soc.* **2002**, *124*, 15180–15181.
[3] C. Chen, W. Gao, Z. Qin, W. Hu, M. Qu, *J. Appl. Phys.* **1991**, *70*, 6277–6279.
[4] C. Chen, M. Qu, W. Hu, X. Zhang, F. Lin, H. Hu, *J. Appl. Phys.* **1991**, *69*, 6114–6116.
[5] D. M. Pasquariello, R. Kershaw, J. D. Passaretti, K. Dwight, A. Wold, *Inorg. Chem.* **1984**, *23*, 872–874.
[6] Y. D. Li, X. L. Li, R. R. He, *J. Am. Chem. Soc.* **2002**, *124*, 1411–1416.
[7] Margolin, R. Rosentsveig, A. Albu-Yaron, R. Popovitz-Biro, R. Teme, *J. Mater. Chem.* **2004**, *14*, 617–624.
[8] K. Oshima, M. Yokoyama, H. Hinode, M. Wakihara, M. Taniguchi, *J. Solid State Chem.* **1986**, *65*, 392–395.
[9] C. Sourisseau, S. P. Gwet, P. Gard, Y. Mathey, *J. Solid State Chem.* **1988**, *72*, 257–271.
[10] P. Gard, F. Cruege, C. Sourisseau, O. Gorochov, *J. Raman Spectrosc.* **1986**, *17*, 283–288.
[11] Y. D. Li, J. P. Ge, *Chem. Commun.* **2003**, 2498–2499.
[12] X. B. Cao, L. Y. Li, Y. Xie, *J. Colloid Interface Sci.* **2004**, *273*, 175–180.
[13] H. Liang, Y. Shimizu, T. Sasaki, H. Umehara, N. Koshizaki, *J. Phys. Chem. B* **2004**, *108*, 9728–9733.
[14] S. M. Zhou, X. H. Zhang, X. M. Meng, X. Fan, S. T. Lee, S. K. Wu, *J. Solid State Chem.* **2005**, *178*, 399–403.
[15] E. Finkman, B. Fisher, *Solid State Commun.* **1984**, *50*, 25–28.
[16] H. S. W. Chang, D. M. Schleich, *J. Solid State Chem.* **1992**, *100*, 62–70.
[17] L. M. Wu, D. K. Seo, *J. Am. Chem. Soc.* **2004**, *126*, 4676–4681.
[18] S. Furuseth, L. Bratts, A. Kjekshus, *Acta Chem. Scand. A* **1975**, *29*, 623–631.
[19] M. E. Fleet, S. L. Harmer, X. Y. Liu, H. W. Nesbitt, *Surface Sci.* **2005**, *584*, 133–145.
[20] G. Q. Shi, C. Li, Y. Q. Liang, *Adv. Mater.* **1999**, *11*, 1145–1146.
[21] J. Brandup, E. H. Immergut (Ed.), *Polymer Handbook*, John Wiley & Sons, New York, **1975**, p.V-23, V-51.
[22] C. Li, G. Q. Shi, Y. Q. Liang, W. Ye, Z. L. Sha, *Polymer* **1997**, *38*, 5023–5026.
[23] C. Li, G. Q. Shi, Y. Q. Liang, Z. L. Sha, *Polymer* **1997**, *38*, 6421–6422.

Received: September 13, 2005
Published Online: December 27, 2005

